Growth of SnO Nanobelts and Dendrites by a Self-Catalytic VLS Process

Marcelo Ornaghi Orlandi and Edson Roberto Leite*

Departamento de Química, Universidade Federal de São Carlos, CEP 13565−905, P.O. Box 676, São Carlos-SP, Brazil

Rosiana Aguiar

Physics Department, University of Augsburg, D-86159 Augsburg, Germany

Jefferson Bettini

Laboratório Nacional de Luz Síncrotron (LNLS), Campinas-SP, Brazil

Elson Longo

Instituto de Química Universidade Estadual Paulista, Araraquara-SP, Brazil

Received: December 6, 2005; In Final Form: February 2, 2006

This article reports on the growth of SnO nanobelts and dendrites by a carbothermal reduction process. The materials were synthesized in a sealed tube furnace at 1210 °C and at 1260 °C for 2 h, in a dynamic nitrogen atmosphere of 40 sccm. After synthesis, gray-black materials were collected downstream in the tube and the samples were characterized by scanning electron microscopy (SEM), transmission electron microscopy (TEM), and energy-dispersive X-ray spectroscopy (EDX). The results showed that the gray-black materials were composed of nanobelts, which grew in the [110] direction of the orthorhombic structure of SnO. Some of the belts also presented dendritic growth. The dendrites grew in the $(1\bar{1}0)$ planes of the SnO structure, and no defects were observed at the junction between the nanobelts and the dendrites. A self-catalytic vapor−liquid−solid (VLS) process was proposed to explain the growth of the SnO nanobelts and dendrites.

Introduction

The synthesis of quasi-one-dimensional structures (1D nanostructures) has attracted the attention of many research groups in the past few years due to the new and/or superior properties presented by small-scale materials. The properties of these nanostructured materials and the theoretical predictions for their applications have become crucial to the future of basic science and technology.

Among these materials, tin dioxide has been a strategic material due to its potential application in many technological areas such as anodes for fuel cells,[1] chemical sensors,[2] optical materials,[3] and electronic devices.[4] Recently, rutile SnO_2 was synthesized into nanobelt morphology by direct[5] and indirect[6] vapor−solid (VS) methods, and SnO was obtained in disk shape by solidification.[7] The VS method is based on a simple evaporation mechanism and allows for the large-scale production of 1D nanostructures. However, this method does not allow for the fine control of nanobelt dimensions. Thus, the vapor−liquid−solid (VLS) method appears to be the most successful mechanism for generating 1D nanostructures such as nanowires and nanotubes with controlled dimensions.[8] The VLS method has been used successfully to synthesize ZnO,[9] ITO,[10] and a large variety of nanostructures. Recently, SnO_2 nanowires were also obtained[11] by a VLS process, but those nanowires had an orthorhombic structure rather than the more common rutile one.

According to the Sn−O phase diagram,[12] the solubility of the oxide phase in liquid metallic tin is very low, indicating that the VLS mechanism can occur in this system. This assumption was used in this work to grow stannous oxide nanostructures by a self-catalytic VLS process. The effect of

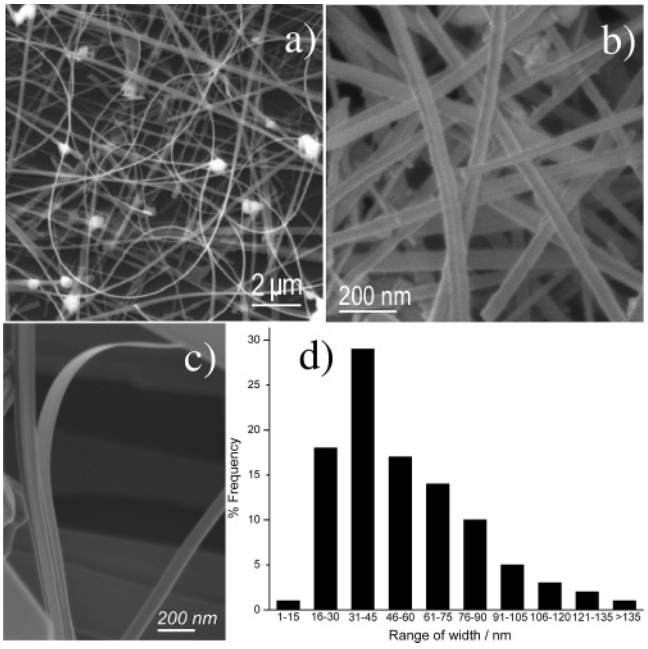

Figure 1. Secondary electron (SE) SEM images showing (a, b) a general view of the as synthesized material, (c) the rectangular cross section of the nanobelts, (d) the histogram of the distribution of widths of the belts.

* Corresponding author. E-mail: derl@power.ufscar.br. Fax: 55 16 3351-8214; Tel: 55 16 3361-5215.

10.1021/jp057099m CCC: $33.50
Published on Web 03/14/2006

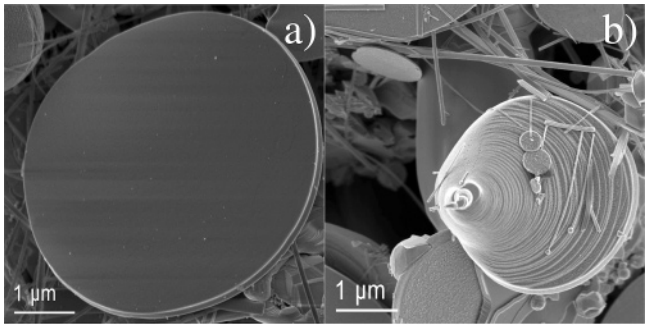

Figure 2. SE-SEM images of (a) SnO flat disks and (b) SnO step disks.

the synthesization temperature on the material obtained was also studied.

Experimental Procedure

The procedure employed to produce the nanobelts was the carbothermal reduction process. In a typical process, an oxide is mixed with any kind of carbon (i.e., carbon black, carbon nanotubes, graphite, etc.) to aid the evaporation process. The main advantage of this method is that materials can be obtained at a lower temperature than if they were produced by a conventional evaporation process. This statement is based on results that have shown that, in the case of many oxides, the lower their state of oxidation the greater their vapor pressure.[12]

In this work, tin monoxide nanostructures were synthesized by a carbothermal evaporation process in a sealed tube furnace. The SnO_2 powder (Aldrich) was mixed with carbon black (Union Carbide) at a molar ratio ([SnO2]/[C]) of 1.5, and this mixture was used as a source material for the synthesis. The mixed powder was put into an alumina boat, which was placed in the hot zone of a tube furnace. The synthesis was carried out at 1210 °C and at 1260 °C for 2 h under a N_2 gas flow of 40 cm^3 min^{-1}. The products obtained after synthesization were characterized by field emission scanning electron microscopy (FE-SEM; Zeiss, Supra 35 at 2 kV), high-resolution transmission electron microscopy (HRTEM; JEOL, 3010 at 300 kV), and energy-dispersive X-ray spectroscopy (EDX) coupled to the

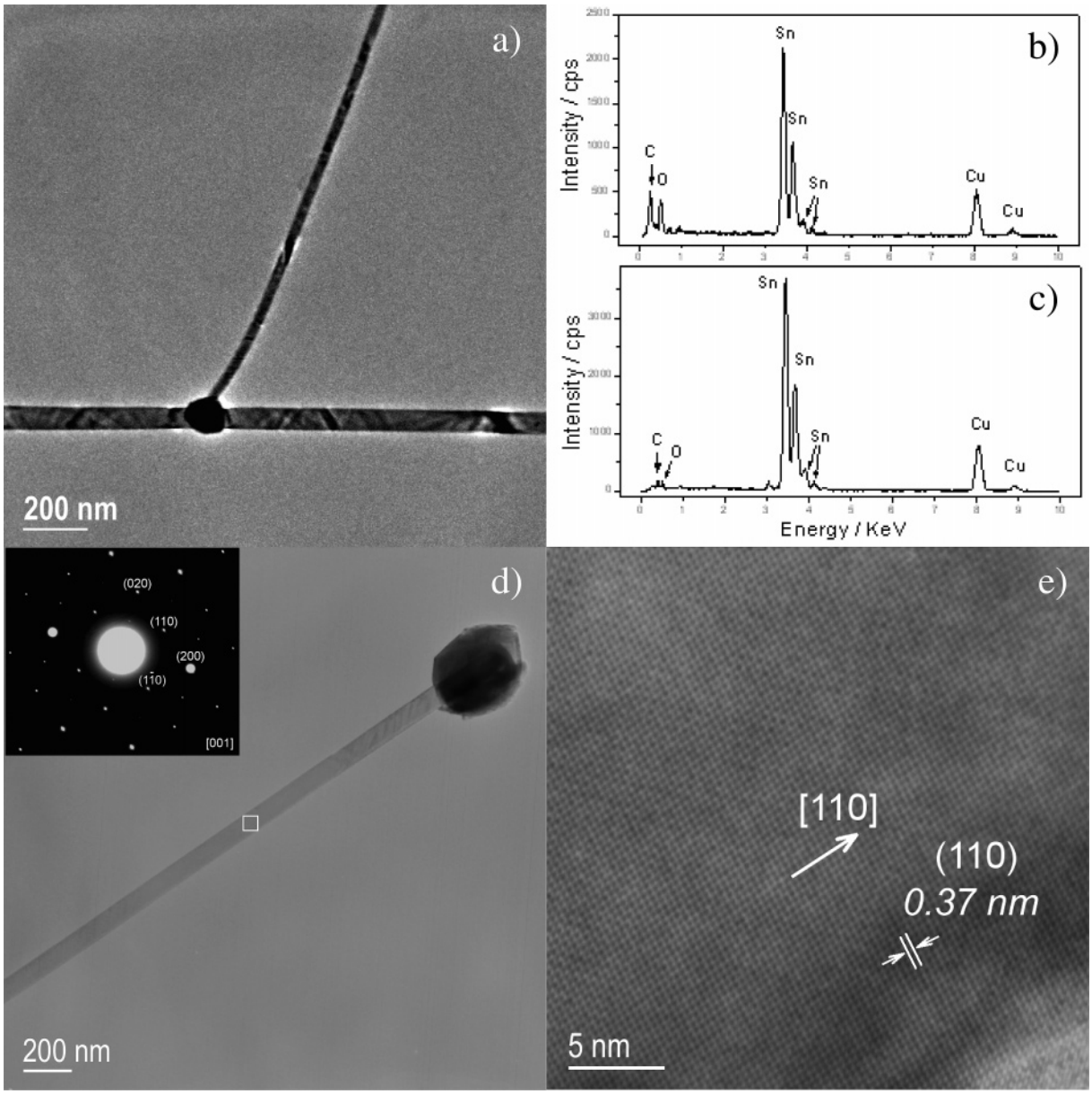

Figure 3. (a) Low magnification TEM image of VLS nanobelts. (b) EDX spectrum of the nanobelt of Figure 4a. (c) EDX spectrum of a metallic tin nanoparticle. (d) Low magnification TEM image of other VLS nanobelt. The inset shows the SAD of the belt. (e) HRTEM image of the SnO VLS-nanobelt marked in (d).

TEM. For the electron microscopy analyses, solutions were prepared with the collected materials in an alcohol medium. For the SEM analyses, a few drops of solution were placed on a flat substrate, and for the TEM analyses two drops of solution were dripped onto a carbon-coated copper grid.

Results and Discussion

The synthesis resulted in gray-black wool-like products that were collected downstream in the region where the temperature ranged from 400 °C to 500 °C, independently of the temperature of synthesization. Figures 1 and 2 show SEM images of the materials synthesized at 1210 °C, consisting of 1D nanostructured materials with rectangular cross-sections (nanobelts; Figures 1a−c), and disklike materials[7] (Figure 2a,b). As indicated in Figure 1, the nanobelts were flat and homogeneous along their length, most of them presenting metallic tin particles at their tips. The presence of tin nanoparticles attached to the tips of the nanobelts is an indication that the VLS method triggers the growth of these belts.[8] Figure 1d shows a histogram depicting the width distribution of the nanobelts, revealing a single modal distribution centered in the range from 31 to 45 nm. The smallest and the largest widths of these nanobelts were 7 and 650 nm, respectively, with about 90% of the nanobelts ranging from 16 to 90 nanometers. The width/thickness ratio for these nanobelts was between 4 and 12. The disks were characterized, revealing results similar to those previously reported by Dai et al.[7] We also found disks with flat surfaces and with spiral steps on the surfaces (Figures 2a,b), and the EDX analyses indicated that their compositions were close to SnO. The SAD analysis confirmed that the disks grew in the tetragonal structure of SnO, which is the same structure as that reported by ref 7. The growth mechanism proposed by Dai[7] for such disks involves a solidification process, but it is still not fully understood. No morphological differences were found between the materials synthesized at 1210 °C and at 1260 °C, and this finding is discussed below.

Figure 3a shows a TEM image of typical SnO nanobelts. It can be observed that these nanobelts have a well-defined shape. Figures 3b,c, which correspond to the EDX analyses of the smaller nanobelt and of the nanoparticle of Figure 3a, respectively, indicated that the nanobelt was composed of Sn and O, while the nanoparticles consisted basically of Sn with a minor concentration of oxygen. These results are strong evidence that nanobelts grow by a VLS process. The carbon and copper peaks in Figures 3b,c are due to the carbon-coated copper grids used for the TEM analyses. Semiquantitative EDX analyses of nanobelts showed a concentration of 49±3 (% atomic) for Sn and of 51±3 (% atomic) for O, which is close to SnO stoichiometry. Figure 3d shows another SnO nanobelt with a metallic drop at its tip, and the inset shows the selected area electron diffraction (SAD) pattern of this belt. The SAD is oriented along the [001] zone axis of the orthorhombic structure of SnO (JCPDS #13.0111), and it shows that the nanobelt is a single crystal. Figure 3e shows a HRTEM image of the SnO nanobelt depicted in Figure 3d, which confirms that the nanobelts are single crystalline and have a low concentration of defects. The interplanar distance of 0.37 nm (Figure 3e) is related to the (110) planes of the SnO structure and derives from the normal growth direction by about 8 degrees, which means SnO nanobelts grow in the [110] direction. As the belt is oriented in the [001] zone axis, the surface plane of the wide surface is the (001) one. The surface of the narrow side of the belt is the $(1\bar{1}0)$ crystallographic plane, as showed by the SAD. Figure 4 schematically illustrates the growth planes of SnO nanobelts.

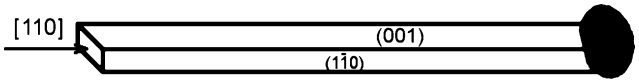

Figure 4. Schematic illustration of growth planes of SnO nanobelts.

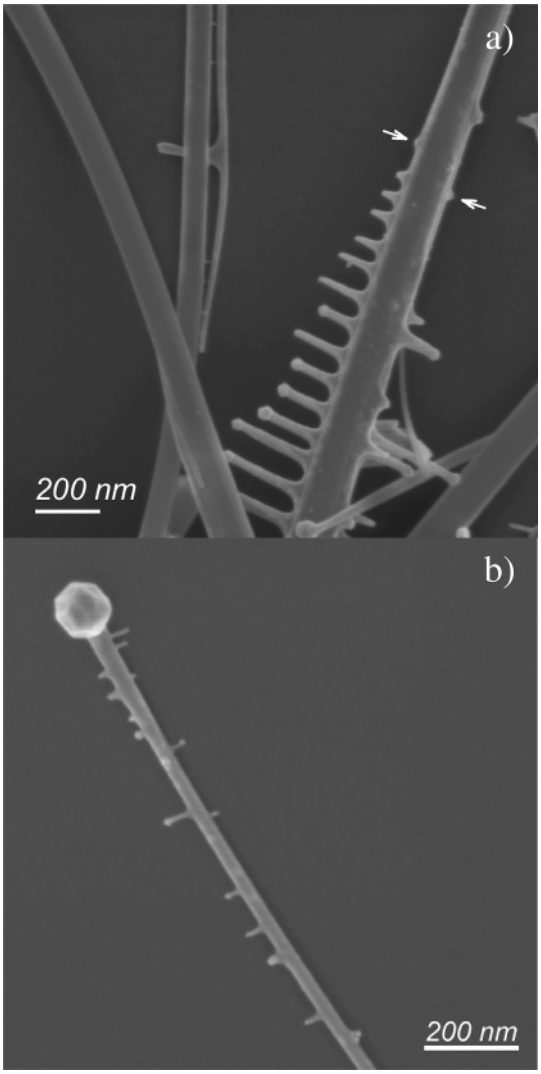

Figure 5. (a, b) SEM images of SnO nanobelts with dendritic growth (the white arrows in part (a) show the initial stage of the dendritic growth).

This is the first report of nanobelts with this structure. A recent paper reported that SnO branches synthesized by the conventional evaporation method grew in the tetragonal structure.[13] This means that the morphology and structure of SnO nanostructures depend on the synthesization conditions. A statistical analysis of the SnO nanobelts' dimensions indicated a correlation between the tin nanoparticle size and the nanobelt width (droplet diameter/nanobelt width = 1−1.5). These findings, together with the distribution shown in Figure 1d, suggest that the VLS method provides good control over nanobelt dimensions.

Dendritic growth was observed in some SnO nanobelts, as presented in the SEM images of Figure 5. These dendrites grew perpendicularly to the growth direction of the nanobelt, and each dendrite also had a droplet at its end, indicating that not only the nanobelts grew by a VLS process but also that these belts can work as substrates for additional growth of dendrites on their surfaces by the same process. The white arrows in Figure 5a show the dendrites' initial stages of growth. Figure 6 shows

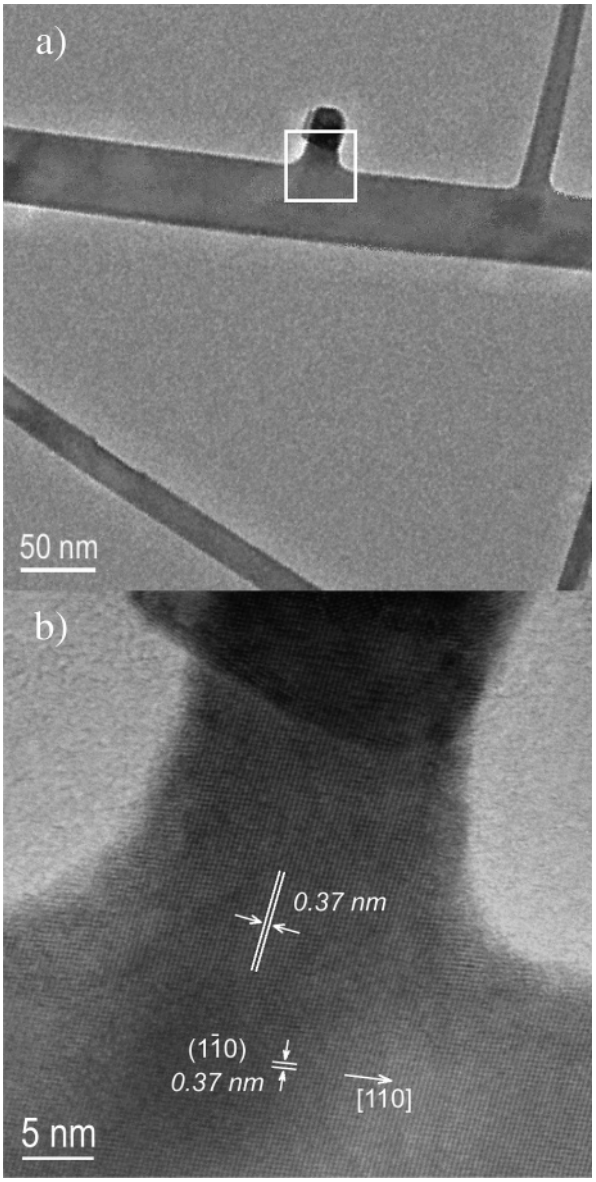

Figure 6. (a) TEM image of a nanobelt presenting dendritic growth and (b) HRTEM image of the junction between the belt and the dendrite presented in (a).

TEM images of a nanobelt with dendrites. No defects were observed at the junction of the nanobelts with the dendrites, as showed in Figure 6b. This means that dendritic growth is oriented by the nanobelts and that the dendrites grow in (1$\bar{1}$0) planes of the SnO structure, which explains the perpendicular growth of dendrites in relation to the growth direction of the nanobelt.

Although the growth mechanism of tin monoxide nanobelts by the VLS process is still not fully understood, we put forward an explanation. We propose that the following chemical reactions occur when a carbothermal reduction process is used:

$$SnO_{2(s)} + C_{(s)} \rightarrow SnO_{(g)} + CO_{(g)} \quad (1)$$

$$SnO_{(g)} + CO_{(g)} \rightarrow Sn^{\circ}_{(l)} + CO_{2(g)} \quad (2)$$

Reaction 1 occurs in the alumina boat in the hot zone of the tube furnace. The products of this reaction are carried downstream (by the N_2 gas flow) to a lower temperature zone, where reaction 2 should occur. Since reactions 1 and 2 occur at 1210 °C and at 1260 °C, and the collected material was formed at the same temperature (400−500 °C region) inside the tube, it follows that the collected material is the same, regardless of the synthesization temperature used. That is why no differences were observed in the synthesized materials at different temperatures. One of the products of reaction 2 is liquid metallic tin, which serves as a preferential site for adsorbing the gas-phase reactant (SnO vapor). The nanobelts nucleate after the liquid becomes supersaturated with reactant material (Figure 7a,b) and grow while reactant vapor is available. This physicochemical process is typical of how the VLS method works. This explanation is plausible, for the EDX analysis of the metallic tin droplet indicated an oxygen concentration in the range of 2−5% (atomic), which is higher than the solubility of oxygen in metallic tin, as proposed by the phase diagram[12] (oxygen solubility lower than 1% (atomic) in the temperature range of 400−500 °C). This finding corroborates the supersaturation step.

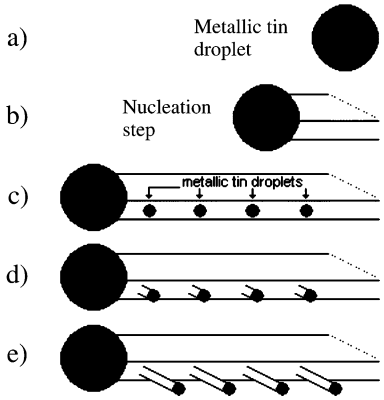

Figure 7. Schematic illustration of the growth mechanism of the SnO nanobelts and dendrites. (a) Liquid metallic tin is formed from the reaction between SnO and CO gases. (b) A nucleation process occurs after the liquid becomes supersaturated with SnO vapor. (c) The nanobelt grows and can serve as substrate for the deposition of small liquid metallic tin droplets. (d, e) These small droplets serve as preferential sites for adsorbing reactant vapor and the nucleation and growth process occurs again, forming dendrites at the nanobelts.

Because no metallic material was put into the tube during the synthesis to act as catalytic material, it is proposed that the SnO nanobelts grow by a self-catalytic VLS process, since the metallic tin is formed by reaction 2 inside the furnace. One advantage of the self-catalytic VLS process is that purer nanobelts can be obtained than those produced by the conventional VLS process, since the droplet has the same chemical elements as the belts. Once the tin droplet is supersaturated and a nucleus is formed, the belt grows with the same structure as that of the initial kernel. It is important to point out that, in a catalytic growth process, a metastable phase such as SnO[12] can be stabilized since the process is controlled kinetically rather than thermodynamically. To explain the dendritic growth found in some nanobelts, we propose that these belts can serve as substrate for additional liquid metallic tin deposition, as shown in Figure 7c. This supposition is plausible since the gray-black material is formed in the 400−500 °C region and metallic tin is liquid above 232 °C. These small droplets have higher energy than the large ones that originate the belt growth and offer a more active site for adsorbing SnO gas. Hence, the processes of supersaturation, nucleation, and growth also occur in the small droplets, generating dendrites (Figures 7d,e). Epitaxial growth can occur in the nucleation step of dendritic growth, and the dendrite may copy the structure of the belt. This explains the fact that no defects were observed at the junctions.

Since wide band gap materials are technologically important, the synthesis of 1D tin monoxide materials with controlled dimensions is crucial for future commercial applications.

Conclusions

In summary, SnO nanobelts were obtained by a self-catalytic VLS process using a carbothermal synthesis approach. The results indicated that the nanobelts were single crystalline and had a width/thickness ratio of 4 to 12. The SAD and HRTEM analyses showed that the SnO nanobelts grew in the [110] direction of the orthorhombic structure of SnO. Some nanobelts presented dendritic growth, and the results showed that the dendrites copied the same orientation of the belts. No defects were formed at the junction between the belt and the dendrite, which must be due to the substrate character of the nanobelts, which favored the epitaxial growth of dendrites. A growth mechanism for the nanobelts and dendrites was also proposed, considering the reaction between SnO(g) and CO(g), which resulted in liquid metallic tin droplets and CO_2 gas. The metallic tin serves as the site for adsorbing the gas-phase reactant (SnO vapor), resulting in the self-catalytic VLS mechanism.

Acknowledgment. The financial backing of the Brazilian agencies FAPESP and CNPq is gratefully acknowledged. The TEM facilities were provided by the LME-LNLS (National Laboratory of Synchrotron Light), Campinas, and by the Institute of Chemistry of UNESP, Araraquara, both in Brazil.

References and Notes

(1) Jiang, L. H.; Sun, G. Q.; Zhou, Z. H. *J. Phys. Chem. B* **2005**, *109*, 8774.

(2) Fagan, F. G.; Amarakoon, V. R. W. *Am. Ceram. Soc. Bull.* **1993**, *72*, 119.

(3) Wu, X.; Zou, B.; Xu, J.; Yu, B.; Tang, G.; Zhang, G.; Chen, W. *Nanostruct. Mater.* **1997**, *8*, 179.

(4) Pianaro, S. A.; Bueno, P. R.; Longo, E.; Varela, J. A. *J. Mater. Sci. Lett.* **1995**, *14*, 692.

(5) Pan, Z. W.; Dai, Z. R.; Wang, Z. L. *Science* **2001**, *291*, 1974.

(6) Leite, E. R.; Gomes, J. W.; Oliveira, M. M.; Lee, E. J. H.; Longo, E.; Varela, J. A.; Paskocimas, C. A.; Boschi, T. M.; Lanciotti, F., Jr.; Pizani, P. S., Jr.; Soares, P. C. *J. Nanosci. Nanotech.* **2002**, *2*, 125.

(7) Dai, Z. R.; Pan, Z. W.; Wang, Z. L. *J. Am. Chem. Soc.* **2002**, *124*, 8673.

(8) (a) Wagner, R. S.; Ellis, W. C.; Arnold, S. M.; Lacjson, K. A. *J. Appl. Phys.* **1964**, *35*, 2993. (b) Morales, A. M.; Lieber, C. M. *Science* **1998**, *279*, 208. (c) Xia, Y.; Yang, P.; Sun, Y.; Wu, Y.; Mayers, B.; Gates, B.; Yin, Y.; Kin, F.; Yan, H. *Adv. Mater.* **2003**, *15*, 353.

(9) Ding, P.; Gao, P. X.; Wang, Z. L. *J. Am. Chem. Soc.* **2004**, *126*, 2066.

(10) Orlandi, M. O.; Aguiar, R.; Lanfredi, A. J. C.; Longo, E.; Varela, J. A.; Leite, E. R. *Appl. Phys. A* **2005**, *80*, 23.

(11) Chen, Y. X.; Campbell, L. J.; Zhou, W. L. *J. Cryst. Growth* **2004**, *270*, 505.

(12) Samsonov, G. V. *The Oxide Handbook*; Plenum Press: New York, 1973.

(13) Wang, Z. L.; Pan, Z. *Adv. Mater.* **2002**, *14*, 1029.